This article has been accepted for publication in a future issue of this journal, but has not been fully edited. Content may change prior to final publication. Citation information: DOI 10.1109/LAWP.2018.2883235, IEEE Antennas and Wireless Propagation Letters

A Proposal to Improve Ray Launching Techniques

Andres Navarro, *Senior Member, IEEE*, Dinael Guevara, *Senior member, IEEE*, and Jorge Gómez, *Senior Member, IEEE*

***Abstract*— In this study, we demonstrate the implementation of an algorithm to model 3D-ray launching. A fixed-size reception sphere and cylinder is used in conjunction with numerical methods to simulate the multipath propagation in a reduced computational time while retaining accuracy. This approach was implemented in a two office environments that were validated previously by the authors in different simulations. The mathematical feasibility of this method in these applications is demonstrated and the obtained results are discussed. The proposed method has been previously validated by authors in different simulations shown in references.**

***Index Terms*—Ray Launching, Channel modeling, Ray Tracing, Propagation.**

I. Introduction

THE 3D ray launching (RL) technique, also known as shooting and bouncing ray technique, is widely used to provide reliable information about the full parameters for wireless channel modeling in indoor and outdoor environments to perform adequate coverage and capacity estimations [1] [2]. However, the computational performance for the RL is highly dependent on the approach of reception sphere technique. For example, with the approach using reception spheres, receivers are assigned to a certain volume in space (typically a sphere), forming the terminal reception sphere. Thus, a launched ray reaches a receiver if it intersects the corresponding reception sphere. The challenge with the conventional approach of using reception spheres is in determining the appropriate sphere size. One solution proposed in literature is the use of adaptive reception spheres based on planar geometry [3] [4]. However, this approach significantly increases the simulation time [5]. Therefore, it is necessary to develop a novel technique based on the reception sphere but with reduced simulation time.

In this study, we propose a novel approach of implementing a fixed-size reception sphere and cylinder in conjunction with numerical methods and a 3D RL model to simulate the multipath propagation in previously validated office environments [6] [7]. The measured and predicted values were subsequently compared to verify the effectiveness of the proposed technique.

II. Reception Sphere

The use of a reception sphere requires that each ray is launched such that it is separated from the neighboring rays by a nearly constant angle of α. A reception sphere with the correct radius can receive only one of the rays. Notably, the radius, *r*, of the reception sphere is proportional to the unfolded path length from the source to the receiver and differs for each ray path [3], as shown in (1).

$$\boldsymbol{r = \alpha d/\sqrt{3}} \tag{1}$$

In addition, direct (line-of-sight) rays, including the reflected, diffracted, and/or transmitted rays, exhibit a $1/d^2$ power dependence, where d represents the total ray path length according to Friis free-space transmission [3].

A power cutoff threshold of −20 dB below the power of the strongest ray is applied to the launched rays to ensure that only effective paths are considered [2]. This procedure is required since the RL paths are determined geometrically. The strongest ray is the direct ray with a minimum path length of d_0. The transmitted, reflected, and diffracted weak rays are considered if their power is greater than or equal to −20 dB below d_0 (i.e., if the path length is less than the maximum path length, d_m). Additionally, if the transmitted, reflected or diffracted loss is Lm, it can be shown that the Friis free-space transmission incurs a cutoff threshold of −20 dB as shown in (2).

$$20log_{10}(d_0) - 20log_{10}(d_m) - Lm = -20dB \tag{2}$$

Equation (2) can also be written as

$$20log_{10}(d_m) = 20log_{10}(d_0) + 20dB - Lm \tag{3}$$

If d_0 is known, the maximum value of the d_m occurs when we have $Lm = 0$; that is when the transmitted, reflected or diffracted ray-path is assumed as a hypothetical path lossless relative to free space. In practice, we have $Lm > 0$; that is when all the transmitted, reflected or diffracted paths are modeled in a real indoor environment. Therefore, all the real path lengths are less than the maximum value of the d_m to a defined cutoff threshold.

A. Navarro is with Universidad Icesi., Cali, Colombia (e-mail: anavarro@icesi.edu.co).

D. Guevara, is with Universidad Francisco de Paula Santander, Cucuta, Colombia. (e-mail: dinaelgi@ufps.edu.co).

J. Gomez is with Universidad del Magdalena, Santa Marta, Colombia (e-mail: jgomez@unimagdalena.edu.co).

This article has been accepted for publication in a future issue of this journal, but has not been fully edited. Content may change prior to final publication. Citation information: DOI 10.1109/LAWP.2018.2883235, IEEE Antennas and Wireless Propagation Letters

If d_0 is known and $Lm = 0$, (3) can be rewritten as follows to ensure that all effective paths are modeled.

$$d_m = 10d_0 \tag{4}$$

Therefore, the radius of the sphere reception associated with maximum path length can be found by substituting (4) into (1):

$$\boldsymbol{r_m = 10\alpha d_0/\sqrt{3}} \tag{5}$$

where r_m is the largest dimension of the fixed-size reception sphere, which ensures a ray hit.

III. Fixed-Size Reception Sphere

Fig. 1 shows a two-dimensional (2D) view of the fixed-size reception sphere and a few neighboring rays that are received. In the figure, $\mathbf{R}$ is a vector from any point on the source to the center point of the reception sphere. $\mathbf{R}_1$ and $\mathbf{R}_2$ are the vectors from any point on the source to the reflection point, where α is the angular resolution between the two neighboring rays, and $\mathbf{R'}_1$and $\mathbf{R'}_2$ are the vectors from the respective reflection points to the points at which the rays intersect the reception sphere. r_1 and r_2 are the minimum Euclidian distances from the ray paths to the reception sphere center. $\mathbf{d}_1$ and $\mathbf{d}_2$ are the vectors from the points of the ray hits on the reception sphere to the tangent points on the exact sphere. P_1 and P_2 are the points of the ray hits on the reception sphere; C and r are the reception sphere center and radius, respectively. $\mathbf{U}_1$ and $\mathbf{U}_2$ are unit vectors of the direction of arrival rays on the reception sphere, α is the angular resolution of two neighboring rays, r_{e1} and r_{e2} are the radii of the correct reception sphere, and r_s is the radius of the fixed-size reception sphere.

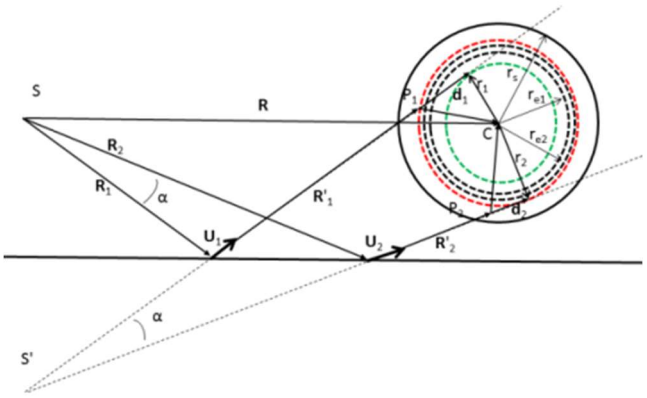

Fig. 1. Two-dimensional schematic of a fixed-size reception sphere.

Once α and $|\mathbf{R}|$ are known, the radius, r_s, of the fixed-size reception sphere shown in Fig. 1 can be found from (6).

$$r_s = 10\,\alpha|\mathbf{R}|/\sqrt{3} \tag{6}$$

If C, P1, and $\mathbf{U}_1$are known, the magnitude of vector $\mathbf{d}_1$ is given as follows:

$$|\mathbf{d}_1| = \overrightarrow{P_1C} \cdot \mathbf{U}_1. \tag{7}$$

Further, r_1 can be calculated as follows:

$$r_1=\sqrt{\left|\overrightarrow{P_1C}\right|^2 - |\mathbf{d}_1|^2}. \tag{8}$$

If $|\mathbf{R}_1|$ and $|\mathbf{R'}_1|$ are known, the radius, r_{e1}, of the correct reception sphere can be found from (1) as follows:

$$r_{e1} = \alpha(|\boldsymbol{R}_1| + |\boldsymbol{R'}_1| + |\boldsymbol{d}_1|)/\sqrt{3}. \tag{9}$$

To determine whether a ray hits a receiver, the following criterion is used:

$$r_1 < r_{e1}. \tag{10}$$

In order to make sure that the phase and length error associate with each ray path is minimized, the length of the ray path from source to the tangent points on the exact sphere can be found from (1) and (9)

$$d = |\boldsymbol{R}_1| + |\boldsymbol{R'}_1| + |\boldsymbol{d}_1| \tag{11}$$

Each ray that is received and meets the criterion is recorded with the length d in a raw RL output file; rays that do not meet the criterion are not considered as received, and the recursive ray path mechanism continues.

IV. Fixed-Reception Cylinder

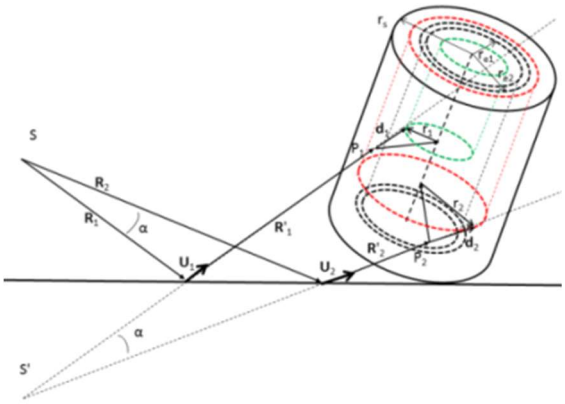

Fig. 2. Three-dimensional schematic of the fixed-size cylinder.

To verify whether the ray hits on the edge of the cylinder and to calculate the corresponding diffraction, we use the concept of a fixed-size cylinder with its longitudinal axis exactly over the edge. The radio of the fixed-size cylinder is as that same given by the fixed-size reception sphere. Fig. 2 shows a three-dimensional (3D) view of the fixed-size cylinder with two received neighbor rays. In the figure, r_1 and r_2 are the minimum Euclidian distances from the ray paths to the cylinder axis. The radius, r_s, of the cylinder can be calculated using (6) and the radius, r_{e1}, of the correct reception cylinder can be calculated from (9). If a ray hits the cylinder and fits the criterion in (10),

This article has been accepted for publication in a future issue of this journal, but has not been fully edited. Content may change prior to final publication. Citation information: DOI 10.1109/LAWP.2018.2883235, IEEE Antennas and Wireless Propagation Letters

it is processed and recorded in the output file. However, if the ray does not meet the criterion, it is not considered a hit and the recursive ray path mechanism continues.

V. Analysis and Results

The proposed technique involving a fixed-size reception sphere in conjunction with the criterion given by (10) was tested in two indoor environments. Figure 3 shows the office indoor environment in the main campus of the Universitat Politècnica de València and Figure 4 shows the 3D indoor model that were described in [6]. Figure 5 shows the room indoor environment in the main campus of the Universidad Politécnica de Cartagena and Figure 6 shows the 3D indoor model that were described in [7].

Fig. 3. Office indoor environment in Valencia.

Fig. 4. 3D Office indoor model for Valencia using the Game Engine.

Fig. 5. Room indoor environment in Cartagena.

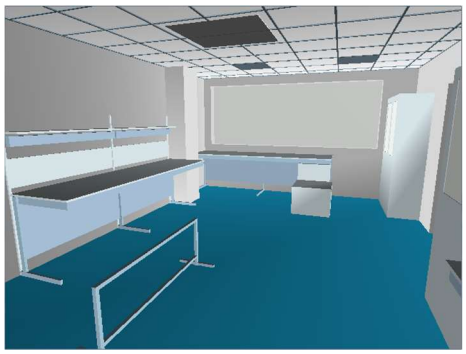

Fig. 6. 3D indoor model for Cartagena using the Game Engine.

Table I shows the software and hardware specifications of the computer where the simulations were executed.

TABLE I. SOFTWARE AND HARDWARE REQUERIMENTS

Software	Operating system	Windows 7-64 bits
	Programming language	Java
	IDE	Eclipse
	Application programming	Open Graphics Library (OpenGL)
	Java native interface binding	Lightweight Java Game Library
	Graphics engine	Java Monkey Engine (jME) V2.0
	Physics engine	Open Dinamic Engines (ODE)
	jME interface to ODE	JME Phisycs 2
	GIS toolkits	Geotools
Hardware	Processor	Intel® Xeon® 2x 8-Core, 2.6GHz
	RAM memory	16GB
	Graphic target	NVIDIA Quadro 4000

Table II shows the computation time required for fixed-size sphere and adaptive sphere models for each scenario.

TABLE II. COMPUTATION TIME

Indoor Scenario	Frequency (GHz)	Shooting Angle (°)	Launched Rays	Processed Rays	Reception Points	Processing Time (hours)	
						Fixed-Size Sphere	Adaptive Sphere
Office	5.4	0.27	655360	404880481	89	5	391
Room	60	0.135	2621440	929330029	20	36	1147

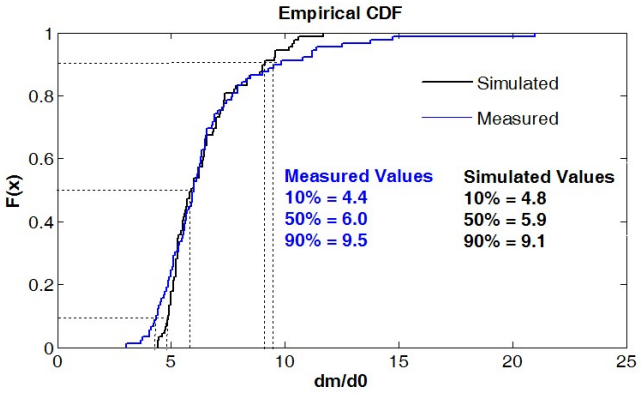

Fig. 7. CDFs of the of the d_m/d_0 values for position 41 in an office at 5 GHz.

This article has been accepted for publication in a future issue of this journal, but has not been fully edited. Content may change prior to final publication. Citation information: DOI 10.1109/LAWP.2018.2883235, IEEE Antennas and Wireless Propagation Letters

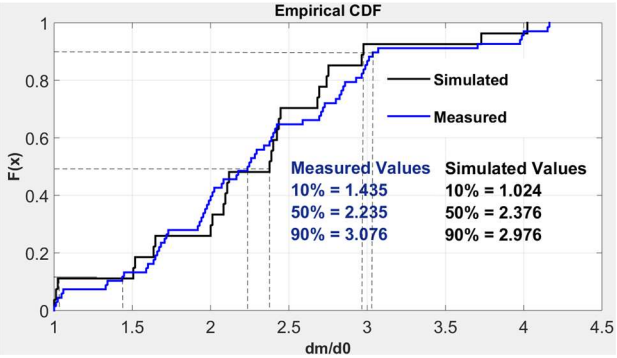

Fig. 8. CDFs of the of the d_m/d_0 values for position 3 in a room at 60 GHz.

The lengths of all ray hits were measured, and the length of the longest ray, d_m, and the Euclidian distance, d_0, from the transmitter to the reception sphere were computed. Then, the d_m/d_0 ratio was calculated. Figs. 7 and 8 show the cumulative distribution functions (CDFs) of the measured and simulated d_m/d_0 values, including the ranges representing 90% of the values from the entire reception sphere fulfilling the criteria given by (4) and (10).

Figs. 9 and 10 shows the measurement and simulated PDP. Table III shows the statistical summary.

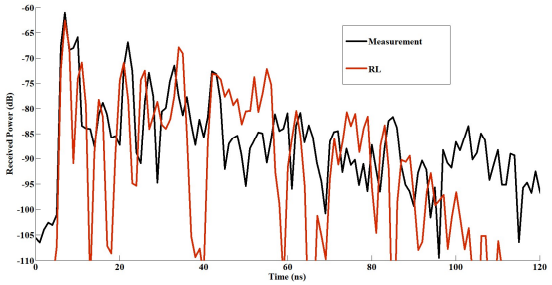

Fig. 9. Measured and simulated PDP for position 41 in an office at 5 GHz.

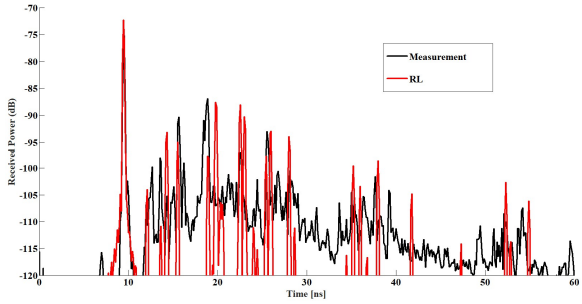

Fig. 10. Measured and simulated PDP for position 3 in a room at 60 GHz

TABLE III. STATISTICAL SUMMARY OF DELAY SPREAD PREDICTION AND PATH LOSS

Indoor Scenario	Frequency (GHz)	Position	RMS (ns)			PL (dB)		
			M	RL	%	M	RL	%
Office	5.4	41	17.2	18.8	91.5	-56.2	-57.1	98.4
Room	60	3	4.19	4.39	95.2	-71.1	-70.8	99.6

VI. CONCLUSIONS

The method proposed in this study involves the application of a reception sphere as the endpoint and a diffraction cylinder to estimate edge diffraction using UTD. The results show that the proposed method considerably improves the computation time, preserving the accuracy of the results obtained in previous studies ([6] and [7]).

REFERENCES

[1] L. Azpilicueta, M. Rawat, K. Rawat, F. M. Ghannouchi, and F. Falcone, "A Ray Launching-Neural Network Approach for Radio Wave Propagation Analysis in Complex Indoor Environments," *IEEE Trans. Antennas Propag.*, vol. 62, no. 5, pp. 2777–2786, May 2014.

[2] J. Weng, X. Tu, Z. Lai, S. Salous, and J. Zhang, "Modelling the mmWave channel based on intelligent ray launching model," *2015 9th European Conference on Antennas and Propagation (EuCAP)*. IEEE, pp. 1–4, 2015.

[3] S. Y. Seidel and T. S. Rappaport, "Site-specific propagation prediction for wireless in-building personal communication system design," *IEEE Trans. Veh. Technol.*, vol. 43, no. 4, pp. 879–891, 1994.

[4] G. Durgin, N. Patwari, and T. S. Rappaport, "An advanced 3D ray launching method for wireless propagation prediction," In *Vehicular Technology Conference, 1997, IEEE 47th*. IEEE, 1997. pp. 785-789.

[5] D. Shi, J. J. Bi, Z. L. Tan, and Y. G. Gao, "Site-specific wave propagation prediction with improved shooting and bouncing ray tracing method," in *2015 1st URSI Atlantic Radio Science Conference (URSI AT-RASC)*, pp. 1–1, 2015

[6] A. Navarro, D. Guevara, D. Escalante, J. Vargas, J. Gómez, N. Cardona, and J. Gimenez, "Delay spread estimation using a game engine ray based model in indoor scenario at 5 GHz", *Journal of Engineering and Applied Sciences*, vol. 11, no. 5, 2016.

[7] PASCUAL-GARCÍA, Juan, et al. On the importance of diffuse scattering model parameterization in indoor wireless channels at mm-wave frequencies. *IEEE Access*, 2016, vol. 4, p. 688-701.